Thermal Unimolecular Elimination of Water from *tert*-Butyl Alcohol: Deuterium Kinetic Isotope Effects, Transition Structure, Reaction Path, and Mechanism

Bansi L. Kalra‡ and David K. Lewis*

Department of Chemistry, Connecticut College, New London, Connecticut 06320

Stephanie R. Singer, Anuradha S. Raghavan, and John E. Baldwin*

Department of Chemistry, Syracuse University, Syracuse, New York 13244

B. Andes Hess, Jr.*

Department of Chemistry, Vanderbilt University, Nashville, Tennessee 37235

Received: September 3, 2004; In Final Form: October 20, 2004

Thermal decomposition of $(CH_3)_2C(OH)CD_3$ in a static reactor and in a shock tube reactor led to intramolecular symmetry-corrected k_H/k_D kinetic isotope effects for eliminations of HOH and HOD of 1.80 ± 0.08 at 436 to 481 °C and 1.54 ± 0.12 at 813 to 883 °C. Calculations with B3LYP/6-31G* theory defined the transition structure for the 1,2-elimination reaction, the internal reaction coordinate path, and k_H/k_D predictions. The reaction takes place through a four-centered transition structure approached through very different progressions of bond length changes along the reaction coordinate.

Introduction

In 1934 Schultz and Kistiakowsky established that the gas-phase thermal decomposition of *tert*-butyl alcohol (TBA) to form 2-methylpropene (MP) and water was a homogeneous unimolecular reaction.[1]

$$\underset{\text{TBA}}{(CH_3)_2C(OH)CH_3} \xrightarrow{-HOH} \underset{\text{MP}}{(CH_3)_2C{=}CH_2}$$

In 1949 Barton and Howlett demonstrated that the gas-phase thermal decomposition of ethyl chloride to form ethylene and hydrogen chloride occurred unambiguously through a unimolecular process.[2] There soon followed numerous additional examples of 1,2-eliminations of water from alkyl alcohols, alcohols from dialkyl ethers,[3] hydrogen halides from alkyl halides, and similar thermal decompositions characterized by clean first-order kinetic behavior and understandable correlations between the structures of starting materials and experimentally determined reaction rates and activation parameters.[4] Pronounced polar effects gave rise to quasiheterolytic formulations for such reactions[3] and electrostatic models for predicting activation energies.[5] Representative examples were demonstrated to be syn eliminations, a stereochemical characteristic consistent with a concerted reaction mechanism.[6] The decompositions were generally considered to involve four-center processes that took place without the intervention of any reactive intermediate.

Orbital symmetry theory[7] and the orbital phase continuity principle[8] had little to say explicitly as to the mechanism of 1,2-eliminations of this type and the related gas-phase unimolecular suprafacial $\sigma^2 + \pi^2$ cycloaddition reactions of alkenes with water, alcohols, and hydrogen halides. Mechanistic inquiry has accordingly not been channeled by theoretical strictures or categories.

Rate constants for the decomposition of TBA to MP and water have been determined as functions of temperature by several groups using either static reactor or shock-tube kinetic methods.[1,9−13] The data from kinetic work using a single-pulse shock tube over the temperature range 920−1175 K provided the Arrhenius activation parameters log A = 14.6 and E_a = 66.2 kcal/mol.[12] Careful comparisons with other work, using several different comparative rate methods, led to the conclusion that the activation energy lies between 63.0 and 66.2 kcal/mol; the higher value was favored, for it gave the best agreement with extrapolations from low-temperature work. A later work under static reactor conditions from 776 to 885 K found the Arrhenius parameters for the unimolecular elimination of water from TBA to be log A = 13.6 and E_a = 64.1 kcal/mol.[13] All of these values agree reasonably with the parameters calculated by O'Neal and Benson based on a semi-ion pair four-centered transition state, log A = 13.6 and E_a = 62.4 kcal/mol.[14]

The thermal decomposition of TBA studied in shock waves over a higher temperature range, 1120−1630 K, provided activation parameters for both the unimolecular process giving water and MP and radical reactions initiated by a homolylic C−C bond cleavage leading from TBA to CH_3 and $(CH_3)_2$-COH.[15] The channel giving radical intermediates had E_a = 81.5 kcal/mol; it was dominated by the molecular decomposition channel giving MP directly, having log A = 14.55 and E_a = 65.4 kcal/mol. From the shock-tube kinetic data secured at 925−1175 K[12] together with the data obtained at 920−1630 K[15] were calculated the parameters log A = 14.55 and E_a = 65.8 kcal/mol over 920−1630 K.[15] Kinetic modeling suggested that above 1750 K the radical channel begins to dominate the decomposition, and corrections for pressure-dependent effects with RRKM theory could well be of significance.[15]

In the present work the decomposition of TBA has been examined more closely through determinations of deuterium kinetic isotope effects and DFT calculations to define the

‡ Permanent address: Department of Chemistry, Hollins University, Roanoke, VA 24020.

10.1021/jp046020v CCC: $27.50
Published on Web 12/07/2004

transition structure for the reaction, the internal reaction coordinate path, and the k_H/k_D ratio. The two approaches provide a detailed picture of the reaction mechanism, one that re-enforces some earlier understandings of this and other concerted four-center eliminations.

Experimental Section

Materials. The substrate, *tert*-butyl alcohol having one of three methyl groups replaced by d_3-methyl (TBA-d_3; $(CH_3)_2C(OH)CD_3$, 98 atom % D) was obtained from Merck, Sharp, and Dohme, Canada. For gas chromatographic identification and calibration purposes, the unlabeled alcohol (TBA; 99.5%) and CP-grade 2-methylpropene (MP**)** were purchased from J. T. Baker and Matheson Gas Products, respectively. All liquid samples were degassed before use through multiple freeze−pump−thaw cycles. The gaseous MP from a lecture bottle was used as obtained. Ultrahigh purity helium (99.999%) was used as the driver gas for the shock-tube runs.

Sample Preparation. A greaseless high vacuum line was used for the preparation of gas mixtures for the shock-tube runs. A 3.2% mixture of $(CH_3)_2C(OH)CD_3$ (TBA-d_3) in argon and a calibration mixture containing 2.0% TBA and 0.84% MP in argon were prepared by transferring known pressures of degassed TBA-d_3 or TBA or MP into a 1-L glass storage bulb and then diluting the compounds with Matheson Research Grade (99.9999%) argon. The gas mixtures were allowed to sit for about 4 days to achieve thorough mixing. For the static reactor runs, the degassed substrate (TBA-d_3) was used without mixing with argon.

Apparatus, Kinetic Runs, and Samples for NMR Analysis. A 2.5-cm i.d. glass single pulse shock tube was used for the high-temperature (1086−1156 K) runs while the low-temperature (709−754 K) runs were carried out in a well-aged 100-cm^3 Pyrex cell surrounded by an aluminum furnace equipped with an Omega 650-J-D digital thermometer. Detailed descriptions and operating procedures for the shock tube and the static reactor have been reported earlier.[16]

For each shock-tube run 50−60 Torr of the 3.2% TBA-d_3 in argon mixture was introduced into the driven section of the tube. The driver section was filled with UHP helium to a pressure sufficient to break an aluminum diaphragm between the two sections, and to send a shock wave through the reaction sample. Immediately after each shock, two samples (25 and 200 mL) of the gaseous products were collected sequentially from the downstream end of the driven section of the shock tube. Both samples contained products produced at the same temperature but over different heating times, 800 and ∼600 μs, respectively.[16,17] The 25-mL sample was used to determine the reaction temperature from the extent of depletion of reactant TBA-d_3. It was analyzed on a Varian 1440-20 gas chromatograph, using a 2-m polypropylene glycol/$AgNO_3$ column at 45−47 °C, and the relative amounts of TBA-d_3 and of (MP-d_3 + MP-d_2) present were determined from the GC peak heights of these compounds, corrected for differences in GC response. The reaction was treated as a homogeneous first-order process with an activation energy of 66.2 kcal/mol and log (A, s^{-1}) of 14.6.[12] The reaction time was taken to be 8×10^{-4} s, the high-temperature "dwell time" previously measured for samples reacting at or near the downstream end of this shock tube.[17]

The 200-mL sample was attached to a vacuum line and cooled to liquid nitrogen temperature for 40−60 min. The argon in the sample was then pumped off very slowly, leaving behind the organic product (MP-d_3 + MP-d_2) and unreacted TBA-d_3. After the removal of argon the sample was warmed to −95 °C in an acetone−liquid nitrogen slush bath for about 30 min. At this temperature, (MP-d_3 + MP-d_2) has a substantial vapor pressure while TBA-d_3 remains condensed. The vaporized (MP-d_3 + MP-d_2) at this temperature was collected in a glass storage bulb cooled in liquid nitrogen, then used for ^{1}H NMR analysis.

TABLE 1: Summary of Reaction Conditions

variable	shock tube	static reactor
reaction pressure (total)	1.2−1.6 atm	0.07−0.13 atm
mixture composition	3.2% TBA-d_3 in Ar	100% TBA-d_3
reaction temp range	1086−1156 K (813−883 °C)	709−754 K (436−481 °C)

TABLE 2: Thermal Decompositions of TBA-d_3 To Form MP-d_3 and MP-d_2

T (°C)	(δ 1.73)/(δ 4.66)	k_H/k_D	MP-d_3 (%)	MP-d_2 (%)
436−442	2.30	1.88	79.0	21.0
459−462	2.34	1.79	78.2	21.8
460−463	2.32	1.83	78.5	21.5
476−481	2.38	1.70	77.3	22.7
813	2.48	1.53	75.4	24.6
869	2.57	1.40	73.7	26.3
879	2.39	1.69	77.2	22.8
883	2.46	1.56	75.7	24.3

For the static reactor runs, the substrate was degassed on a vacuum line connected to the reaction cell and expanded directly into the heated cell. Samples at pressures between 20 and 40 Torr were heated for 1.5−5.5 h. At the end of the heating period the products were transferred to a 25-mL glass bulb; the (MP-d_3 + MP-d_2) product was distilled from a −95 °C bath into a glass storage bulb cooled with liquid nitrogen and subsequently analyzed by ^{1}H NMR.

A summary of the experimental conditions is given in Table 1.

NMR Analyses. The NMR T_1 transverse relaxation times for vinyl hydrogens (at δ 4.66) and methyl hydrogens (at δ 1.73) in isobutylene (2-methylpropene; MP) were measured on a 500-MHz instrument, using an inverse recovery pulse sequence, and found to be 18.9 and 11.4 s, respectively. Determinations of relative absorption intensities for these two resonance signals in samples of (MP-d_3 + MP-d_2) obtained as products from thermal decompositions of TBA-d_3 were made with a pulse delay time of 120 s.[18] The reactions and product analyses are summarized in Table 2.

Experimental Results

The decomposition of TBA-d_3 might involve the formation of HOH and 2-(d_3-methyl)propene (MP-d_3) or the formation of HOD and 1,1-d_2-2-methylpropene (MP-d_2). These two alternatives would involve cleavage of a carbon−hydrogen or a carbon−deuterium single bond. A primary k_H/k_D effect compounded by smaller secondary deuterium kinetic isotope effects would be expected. Were the experimentally accessible k_H/k_D effect a good match to theory-based predictions, the insights provided by theory on the transition structure and the mechanism of the 1,2-elimination process could be viewed with increased confidence, and vice versa.

$$\underset{\text{TBA-}d_3}{(CD_3)(CH_3)C(OH)CH_3} \xrightarrow{-HOH} \underset{\text{MP-}d_3}{(CD_3)(CH_3)C{=}CH_2}$$

$$\underset{\text{TBA-}d_3}{(CH_3)_2C(OH)CD_3} \xrightarrow{-HOD} \underset{\text{MP-}d_2}{(CH_3)_2C{=}CD_2}$$

The number of vinyl protons in the mixture of MP-d_3 and MP-d_2 formed would be proportional to $2 \times 2k_H$, for two methyl

groups might provide the hydrogen to be transferred in the elimination. Formation of MP-d_3 would contribute $3 \times 2k_H$ methyl hydrogens while MP-d_2 would give $6k_D$ methyl hydrogens. Thus the ratio r of integrated proton NMR absorptions for methyl hydrogens in (MP-d_3 + MP-d_2) to vinyl hydrogens in the mixture would be

$$r = (3 \times 2k_H + 6k_D)/(2 \times 2k_H) = 6(k_H + k_D)/(4k_H) \quad (1)$$

and the k_H/k_D ratio of rate constants per hydrogen or deuterium available for transfer could be derived by using eq 2.

$$k_H/k_D = 3/(2r - 3) \quad (2)$$

From the ratio of integrated proton NMR absorptions for methyl versus vinyl hydrogens in (MP-d_3 + MP-d_2) present in product mixtures (column 2 of Table 2) one can calculate symmetry-corrected k_H/k_D ratios (column 3) and then the proportions of MP-d_3 and MP-d_2 in each product mixture. The four thermal decomposition runs conducted in a static reactor gave an average MP-d_3 proportion of (78.3 ± 0.7)%. The four shock-tube runs at higher temperatures gave an average MP-d_3 proportion of (75.5 ± 1.4)%. These uncertainties are not unreasonable for the NMR analytical method employed, though one (as always) would prefer smaller probable errors. The scatter apparent in plots of $\ln(k_H/k_D)$ versus T^{-1} is magnified by an unfavorable relationship between experimental uncertainties in the intensity ratios for δ 1.73 and δ 4.66 proton NMR resonance absorptions and the corresponding uncertainties in the derived k_H/k_D ratios. For example, if a measured NMR intensity ratio were 2.30 ± 0.05 (relative error 2.2%) then the uncertainty in k_H/k_D would be 1.88 ± 0.12 (relative error 6.4%).

The k_H/k_D values derived from the NMR analyses are 1.80 ± 0.08 at 436 to 481 °C and 1.54 ± 0.12 at 813 to 883 °C. These k_H/k_D values and estimated errors based on four measurements at each temperature, when compared using Student's t distribution, are different at the 99% confidence level.[19] There is a slight diminution of the symmetry-corrected k_H/k_D ratio at higher temperatures. There is not a large temperature dependence for the primary deuterium kinetic isotope effect being measured.

Calculational Results

Information about the transition structure for the 1,2-elimination of water from *tert*-butyl alcohol (TBA), the internal reaction coordinate (IRC) pathway linking it with the starting material, and the intramolecular deuterium kinetic isotope effects expected for dehydrations of 2-(d_3-methyl)propan-2-ol (TBA-d_3) was sought through calculations with Gaussian 98W.[20] The B3LYP/6-31G* density functional method, implementation, and basis set were used.[21,22] Second derivatives were calculated to characterize all stationary points. Unscaled B3LYP/6-31G* frequencies obtained analytically provided zero-point energies. A theory-based reaction profile was defined through IRC calculations.

The transition structure (TS) for the thermal elimination of water from TBA was found without difficulty. That it is the transition structure was verified by using the IRC method of following reaction pathways. In Figure 1 are views of TS and of the reactant (TBA), as well as of one additional transition structure (TBATS) that was found, one encountered through a degenerate rotational isomerization about the C2−Cl bond. The barrier to rotation is only 3.1 kcal/mol. The calculated activation energy including zero-point energy corrections for the thermal dehydration of TBA is 63.4 kcal/mol. Other perspectives on TS are provided in Figure 2.

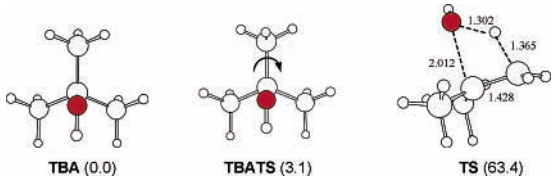

Figure 1. Chem 3D structures for TBA, TBATS, and TS. Distances are given in Å and relative energies (in parentheses) in kcal/mol.

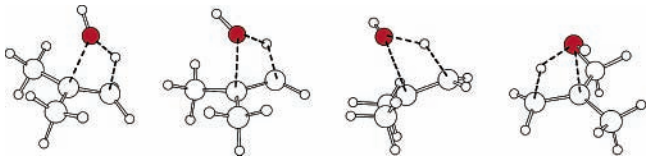

Figure 2. Chem 3D structures showing different views of TS.

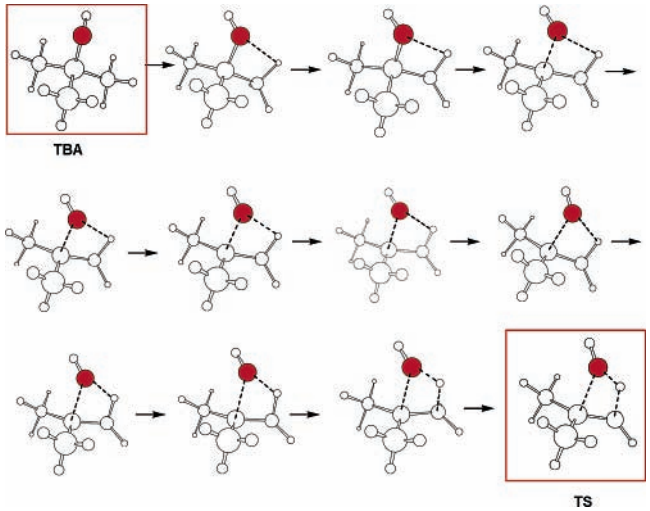

Figure 3. Structural changes along the IRC path from TBA to TS.

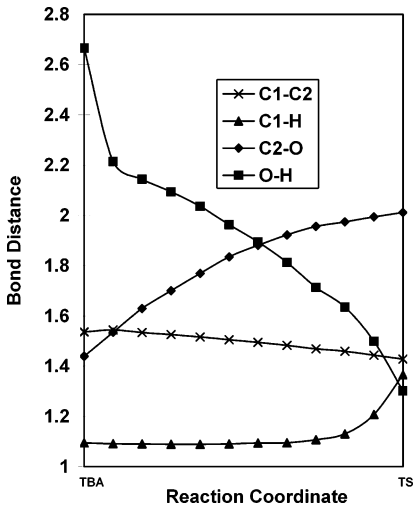

Figure 4. Plot of four critical bond distances at 6 kcal/mol intervals. Bond distances are given in Å.

Figure 3 highlights structural changes for TBA as it progresses along the reaction coordinate to TS. Another representation of changes in molecular structure is provided in Figure 4, one that plots C2−C1, C1−H, C2−O, and O−H bond lengths at six kcal/mol intervals as TBA follows the IRC path toward the transition structure. The C−O length increases substantially, from 1.439 to 2.012 Å, the C2−Cl length shortens, from 1.536 to 1.428 Å, the C−H bond grows longer, from 1.098 to 1.365 Å, whereas the forming O−H bond shortens substantially from 2.666 to 1.302 Å.

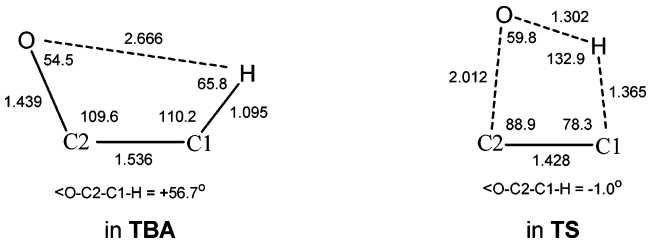

Figure 5. Structural comparisons between O−C2−C1−H in TBA and in TS. Angles are in deg and distances in Å. Below each structure is given the dihedral angle.

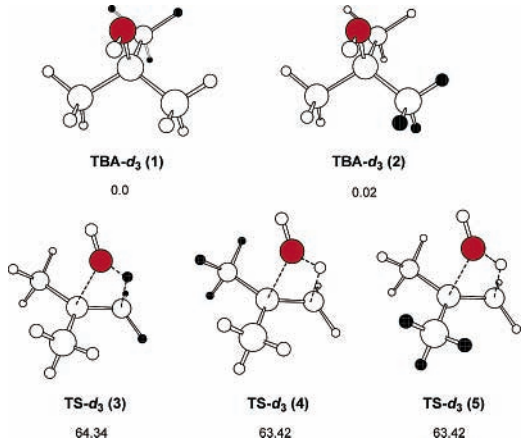

Figure 6. Chem 3D structures for deuterium-labeled options open to starting material TBA-d_3 (**1** and **2**) and to TS-d_3 **(3, 4** and **5**). Energies (with zero-point energies taken into account) at 460 °C are given below each structure in kcal/mol. Deuterium atoms are shown in black.

The initial steep drop of the O−H bond (shortening) is due primarily to a rotation about the C2−C1 bond. The C2−C1 bond length at the transition structure is about halfway along toward the C═C bond length in MP, 1.32 Å. The progressive variations in bond length changes are not simply proportional to each other along the reaction coordinate. Elongation of the C−O bond and shortening of the forming O−H bond lead the way, followed by changes in C2−Cl and finally C1−H.

The structural changes from TBA to TS are shown in yet another fashion in Figure 5, to emphasize the O−C2−C1−H four-atom array in TBA, which becomes the four-atom quadrilateral in TS essential to the elimination process. There are significant reductions in O−C2−Cl and C2−C1−H bond angles, and the O−H−Cl angle is far from linear (see below). The four-center core of the transition structure is essentially planar with a dihedral angle (O−C2−C1−H) of only −1°.

The structures of various deuterium-labeled compounds used in isotope effect calculations are shown in Figure 6 together with calculated energies (in kcal/mol). There are two possible dispositions of the deuterium-labeled methyl group in the starting material; one of these has a symmetry-related equivalent. There are three transition structure alternatives for dehydrations, one leading to HOD and 1,1-d_2-2-methylpropene (MP-d_2), the second two leading to HOH and 2-(d_3-methyl)propene (MP-d_3).

The calculated energies of structures TBA-d_3 (**1**) and TBA-d_3 (**2**) differ by less than 0.02 kcal/mol, a difference taken to be insignificant. The thermal elimination of HOH is favored over elimination of HOD by a statistical factor of 2 and by a lower activation energy. The energy of structures TS-d_3 (**4**) and TS-d_3 (**5**) is 0.92 kcal/mol lower than the energy of structure TS-d_3 (**3**). The calculated activation energies for loss of HOH and HOD (Figure 6) are 63.42 and 64.34 kca1/mol, respectively. The calculated symmetry-corrected k_H/k_D ratio is 1.93 at 460 °C. At 860 °C the calculated k_H/k_D ratio is 1.44.

Discussion and Conclusions

The intramolecular k_H/k_D effect found for the decomposition of TBA-d_3 is comparable with values found for related 1,2-elimination reactions. The reaction of *tert*-butyl ethyl ether to give ethanol and 2-methylpropene is 2.15 times faster than the decomposition of *tert*-butyl-d_9 ethyl ether to give 2-methylpropene-d_8 at 555 °C.[23] Presumably the primary isotope effect is augmented by small secondary effects contributed by the additional deuterium atoms in the system. This finding by Kwart and Stanulonis was interpreted as evidence for considerable C−O bond extension preceding the actual H transfer, a linear H transfer through a quantum-mechanical tunneling process uninfluenced by zero-point energy factors, and a triangular transition state.[23]

The dehydration of chemically activated $CH_2DCH_2OH^*$ takes place with a k_H/k_D intramolecular isotope effect adjusted for the reaction path degeneracy of 1.8 ± 0.4.[24] The calculated RRKM value for the k_H/k_D effect is 1.6. These effects were ascribed primarily to differences in zero-point energies.

The experimentally determined intramolecular k_H/k_D effects, 1.80 ± 0.08 at 436 to 481 °C and 1.54 ± 0.12 at 813 to 883 °C, agree well with the calculated symmetry-corrected k_H/k_D ratios, 1.93 at 460 °C and 1.44 at 860 °C. The match between experimental[12] and calculated activation energies, 66. 2 and 63.4 kcal/mol, respectively, is also in fine agreement.[25] The agreement is actually better than it appears, since the computed value ought to represent the passage of molecules over the very lowest saddle point of the barrier, whereas the experimental value is based on an ensemble average of molecules reacting at significant rates and in some cases passing over a somewhat higher part of the barrier due to vibrational distortions. The agreement between both k_H/k_D and E_a observables and the DFT based values provides a reassuring point of departure for considering the implications for reaction mechanism provided by the theory-derived TS geometry and the IRC path.

The four-centered quadrilateral in TS shown in Figure 5 features an extended C2−O bond (2.012 Å), a strongly reduced C2−C1−H bond angle (to 78.3°), and nearly equal distances separating the forming O−H and the breaking C1−H bonds (1.303 and 1.365 Å). The geometry is similar to but also tellingly different from the transition structure found for the thermal dehydration of ethanol.[25−27] Here the same key structural parameters are calculated to be 1.860 Å, 74.4°, 1.254 Å, and 1.433 Å.[26] The 1,2-elimination of water from TBA versus the similar reaction of ethanol has at the transition state region a longer C2−O bond, reflecting a smaller heterolytic bond dissociation energy and more charge polarization. The abstraction of H by the nucleophilic oxygen in TS requires less elongation of C1−H (0.068 Å less) and less compression of the C2−C1−H bond angle and not as close an approach to the H (by 0.048 Å).

Another insight as to the reaction mechanism is provided by the changes in bond lengths summarized in Figure 4. The plots of bond lengths versus progress along the reaction coordinate underscore the essential changes leading to the transition structure: the distance separating the oxygen atom and the hydrogen that will eventually be abstracted grows shorter and shorter, and the C2−O bond gets longer and longer until, finally, just before the transition region is attained, the C1−H bond begins to weaken and lengthen. The changes in C2−O and the forming O−H bond lengths along the reaction coordinate drive

the reaction. The nucleophilic oxygen abstracts H from C1 when it is close enough and has separated enough from C2. The H−C1−C2 sub-structure as TBA progresses toward TS constricts in bond angle, C1−C2 becomes slightly shorter, and C1−H becomes slightly longer. It is, compared with the C2−O- - -H atoms, relatively passive until the end is near.

Acknowledgment. We thank the National Science Foundation for support of this work through grants CHE-9714356 and CHE-0213374 at Connecticut College and CHE-9902184 and CHE-0211120 at Syracuse University. B.L.K. also thanks Hollins University for partial support.

Supporting Information Available: Geometries, total energies, and zero-point energy corrections for TBA, TBATS, and TS. This material is available free of charge via the Internet at http://pubs.acs.org.

References and Notes

(1) Schultz, R. F.; Kistiakowsky, G. B. *J. Am. Chem. Soc.* **1934**, *56*, 395−398.

(2) Barton, D. H. R.; Howlett, K. E. *J. Chem. Soc.* **1949**, 165−169.

(3) (a) Daly, N. J.; Wentrup, C. *Aust. J. Chem.* **1968**, *21*, 1535−1539. (b) Daly, N. J.; Wentrup, C. *Aust. J. Chem.* **1968**, *21*, 2711−2716.

(4) (a) Maccoll, A.; Thomas, P. J. *Nature* **1955**, *176*, 392−393. (b) Maccoll, A. *Theoretical Organic Chemistry*; Butterworth: London, UK, 1958; pp 230−249. (c) Maccoll, A.; Thomas, P. J. *Prog. React. Kinet.* **1967**, *4*, 119−148. (d) Maccoll, A. *Chem. Rev.* **1969**, *69*, 33−60.

(5) (a) Benson, S. W.; Bose, A. N. *J. Chem. Phys.* **1963**, *39*, 3463−3473. (b) Benson, S. W.; Haugen, G. R. *J. Am. Chem. Soc.* **1965**, *87*, 4036−4044.

(6) Paisley, S. D.; Holmes, B. E. *J. Phys. Chem.* **1983**, *87*, 3042−3048.

(7) (a) Woodward, R. B.; Hoffmann, R. *Angew. Chem., Int. Ed. Engl.* **1969**, *8*, 781−853. (b) Woodward, R. B.; Hoffmann, R. *The Conservation of Orbital Symmetry*; Verlag Chemie: Weinheim, Germany, 1971.

(8) Goddard, W. A. *J. Am. Chem. Soc.* **1972**, *94*, 793−807.

(9) Barnard, J. A. *Trans. Faraday Soc.* **1959**, *55*, 947−951.

(10) Tsang, W. *J. Chem. Phys.* **1964**, *40*, 1498−1505.

(11) Dorko, E. A.; McGhee, D. B.; Painter, C. E.; Caponecchi, A. J.; Crossley, R. W. *J. Phys. Chem.* **1971**, *75*, 2526−2530.

(12) Lewis, D.; Keil, M.; Sarr, M. *J. Am. Chem. Soc.* **1974**, *96*, 4398−4404.

(13) Johnson, W. D. *Aust. J. Chem.* **1975**, *28*, 1725−1731.

(14) O'Neal, H. E.; Benson, S. W. *J. Phys. Chem.* **1967**, *71*, 2903−2921.

(15) Choudhuray, T. K.; Lin, M. C.; Lin, C.-Y.; Sander, W. A. *Combust. Sci. Technol.* **1990**, *71*, 219−232.

(16) (a) Lewis, D. K.; Giesler, S. E.; Brown, M. S. *Int. J. Chem. Kinet.* **1978**, *10*, 277−294. (b) Lewis, D. K.; Bergman, J.; Manjoney, R.; Paddock, R.; Kalra, B. L. *J. Phys. Chem.* **1984**, *88*, 4112−4116.

(17) Lewis, D. K.; Baldwin, J. E.; Cianciosi, S. J. *J. Phys. Chem.* **1990**, *94*, 7464−7467.

(18) Claridge, T. D. W. *High-Resolution NMR Techniques in Organic Chemistry*; Pergamon: Amsterdam, The Netherlands, 1999; pp 114−116.

(19) Fischer, R. B.; Peters, D. G. *A Brief Introduction to Quantitative Chemical Analysis*; W. B. Saunders: Philadelphia, PA, 1969; pp 78−80.

(20) Frisch, M. J.; Trucks, G. W.; Schlegel, H. B.; Scuseria, G. E.; Robb, M. A.; Cheeseman, J. R.; Zakrzewski, V. G.; Montgomery, J. A.; Stratmann, R. E.; Burant, J. C.; Dapprich, S.; Millam, J. M.; Daniels, A. D.; Kudin, K. N.; Strain, M. C.; Farkas, O.; Tomasi, J.; Barone, V.; Cossi, M.; Cammi, R.; Mennucci, B.; Pomelli, C.; Adamo, C.; Clifford, S.; Ochterski, J.; Petersson, G. A.; Ayala, P. Y.; Cui, Q.; Morokuma, K.; Malick, D. K.; Rabuck, A. D.; Raghavachari, K.; Foresman, J. B.; Cioslowski, J.; Ortiz, J. V.; Stefanov, B. B.; Liu, G.; Liashenko, A.; Piskorz, P.; Komaromi, I.; Gomperts, R.; Martin, R. L.; Fox, D. J.; Keith, T.; Al-Laham, M. A.; Peng, C. Y.; Nanayakkara, A.; Gonzalez, C.; Challacombe, M.; Gill, P. M. W.; Johnson, B. G.; Chen, W.; Wong, M. W.; Andres, J. L.; Head-Gordon, M.; Replogle, E. S.; Pople, J. A. *Gaussian 98*, Revision A.7; Gaussian, Inc.: Pittsburgh, PA, 1998.

(21) Becke, A. D. *J. Chem. Phys.* **1993**, *98*, 5648−5652.

(22) Lee, C.; Yang, W.; Parr, R. G. *Phys. Rev. B* **1988**, *37*, 785−789.

(23) Kwart, H.; Stanulonis, J. J. *J. Am. Chem. Soc.* **1976**, *98*, 5249−5253.

(24) Butkovskaya, N. I.; Setser, D. W. *J. Chem. Phys.* **1996**, *105*, 8064−8074.

(25) Another recent theory-based estimate gave an E_a value of 66.6 kcal/mol for the homogeneous thermal loss of water from ethanol; see: Park, J.; Zhu, R. S.; Lin, M. C. *J. Chem. Phys.* **2002**, *117*, 3224−3231.

(26) Butkovskaya, N. I.; Zhao, Y.; Setser, D. W. *J. Phys. Chem.* **1994**, *98*, 10779−10786.

(27) For calculated transition structures for both 1,2-elimination reactions available to 2-fluoroethanol, see: Rajakumar, B.; Reddy, K. P. J.; Arunan, E. *J. Phys. Chem. A* **2003**, *107*, 9782−9793.